

NATIONAL RADIO ASTRONOMY OBSERVATORY  
SOCORRO, NEW MEXICO  
VERY LARGE ARRAY PROGRAM

VLA ELECTRONICS MEMORANDUM NO. 188

AN EXPERIMENTAL TEST OF THE RESPONSE  
OF THE VLA TO AN INTERFERING SIGNAL

A. R. Thompson and T. M. Percival

October 1979

## 1.0 INTRODUCTION

Calculations of the response of the VLA to a steady interfering signal were described in VLA Electronics Memorandum No. 183, and were undertaken in preparation for a workshop on the effects of the proposed Satellite Power System (SPS), for solar energy collection, on radio astronomy. Whether the SPS is eventually implemented or not, the possibility of occurrence of steady interfering signals from other synchronous satellites will certainly increase in the future. Thus it is important to understand the effects of such signals so that harmful interference levels for the VLA and similar synthesis instruments can be specified. Towards this end it was deemed desirable to test some of the predictions of VLA EM No. 183 experimentally, to determine how well the response of the array is understood.

The test described here consisted of mapping a radio source in the presence of a steady cw interfering signal. The signal was transmitted from the Langmuir Laboratory on South Baldy in the Magdalena Mountains, 40 km east of the VLA Site. This allowed a test of the predictions of the effect referred to as fringe-frequency averaging in VLA EM No. 183. The following points were examined.

- 1) The interference pattern in a synthesized map should show structure elongated in the east-west direction. This is because

the interference from a stationary source produces a signal at the correlator outputs which varies at the natural fringe frequency for the source under investigation. Averaging in the (u,v)-plane strongly reduces the interference, except near the v-axis where the fringe frequency goes to zero. The stationary nature of the interfering source is similar to that of a source at the pole, and the east-west structure can also be thought of as distant ring-shaped grating lobes from such a source.

(2) If cell averaging is used to interpolate the visibility onto a rectangular grid of points in the (u,v)-plane, the rms level of the interference should be proportional to  $\Delta u^{-1/2}$ , where  $\Delta u$  is the cell dimension which is assumed equal in both the u and v directions. It should also be possible to test the effect of interpolation by Gaussian convolution.

(3) The response of the array to an interfering signal should be less than that to a source in the main beam of the antennas by a factor  $(\omega_0 \Delta u \cos \delta)^{-1/2}$ , and by the ratio of the gain in the far side lobes to the gain in the main beam. Here  $\omega_0$  is the angular velocity of the earth in  $\text{rad s}^{-1}$ ,  $\Delta u$  is in wavelengths, and  $\delta$  is the declination of the source under observation. The expected amplitude of the interference cannot be calculated because the gain of the antennas in the far side lobes is not known; however, one can see if the observed amplitude leads to a reasonable value for the side lobe gain.

(4) Some idea of the tolerable ratio of rms interference to noise should be obtainable from the probability distribution of the interference amplitude in the map.

## 2.0 THE EXPERIMENT

The transmitted signal at 1427 MHz was derived from a Polarad 1105 B-L signal generator, the frequency of which was monitored by an E.I.P. 351c counter through a Narda 3040-10 coupler. An open-ended L-band waveguide was used as a transmitting horn and a radiated power level of  $1.0 \pm 0.1$  mW was maintained during the experi-

ment. The power level was adjusted using an H.P. 435A/8482A power meter, and an H.P. 8496B switchable attenuator was used to turn the signal on and off as required. The horn was set up in the cupola at the top of the Langmuir Lab, and pointed just west of the array center at a bearing of approximately  $280^\circ$ , with the E-plane horizontal. This resulted in good uniformity of signal strength over the array, which extended mainly along the west arm. Signal strength at the array site was monitored using a horn of aperture 34.5 cm (E-plane)  $\times$  42.6 cm (H-plane) for which the aperture efficiency was taken to be 0.6. This was connected to a Tektronics spectrum analyzer via an Avantek 8199 amplifier with gain 25.8 dB (including the interconnecting cable). The following signal levels were measured at various points on the array during the week preceding the observation:

AW3	-78 dBm	CN7	-71 dBm
AW4	<-90 dBm	DE1	-77 dBm
AW6	-77 dBm	CE9	-79 dBm
AW8	-77 dBm	Visitors' gallery of	
CN5	-77 dBm	Control Building	-77 dBm

AW4 is the only antenna station for which there was not a direct sight path to South Baldy. The reason for the high level at CN7 is not known, but is not important since the antenna at that location was not usable.

During the observation the signal level at the Control Building was measured as -78 dBm, which corresponds to  $-123.3 \text{ dB Wm}^{-2}$ . The expected strength was  $-128 \text{ dB Wm}^{-2}$ , based on a radiated power level of 1.0 mW, an antenna gain of 5 dB and a distance 40.6 km from the array center. The calculated value is probably more reliable since the signal-strength measurements at the site were made fairly close to ground level (from the back of a pickup truck) and ground reflections may have caused some errors. The mean of the two estimates,  $125.7 \pm 2.4 \text{ dB Wm}^{-2}$  was used in analyzing the results.

The observation was made on 1979 July 22 from 01<sup>h</sup> to 11<sup>h</sup> LST. For each 20-minute interval the source to be mapped, 0537+531, was observed for 15 minutes and a calibrator, 0552+398, was observed for the remaining five minutes. A flux density of 1.61 Jy was used for 0552+398. The interfering signal was turned off during each observation of the calibrator to simplify the interpretation of the results. A 10-second record length was used in filling the data base. Fourteen antennas were in use, at stations AW1, AW2, AW3, AW5, AW7, AW8, DN2, DN4, DN6, DE3, CE2, CE6, CE8, and CE9. The observing bandwidth was 12 MHz and the center frequency 1430 MHz. Just over one hour was lost from 08<sup>h</sup>37 to 09<sup>h</sup>42 LST as a result of correlator malfunction, and a corresponding gap can be seen in the (u,v)-coverage shown in Figure 1.

### 3.0 RESULTS

A number of maps were made using the cell averaging technique, with different values of  $\Delta u$ . A quadrant of one of them is shown in Figure 2, and the expected east-west structure in the interference is clearly visible. To be precise, the structure in Figure 2 makes an angle of about 1° with east-west, but an exact east-west alignment is hardly to be expected since the points of occurrence of high visibility amplitudes will also depend upon such things as antenna side lobe structure and interruptions in the source observation to go to the calibrator.

Estimates of the rms interference level in each of the maps were obtained by analyzing the line printer output values for 1200 points in three 20 x 20 squares. Choice of location of these areas within a map was based on a subjective attempt to obtain a representative sample of the interference, and this procedure, no doubt, resulted in some error in the rms levels. The results are listed in Table I and have been corrected for the taper resulting from the interpolation process. In the maps which were analyzed, the point source 0537+531 was subtracted to avoid confusion between interference and side lobes of the source. Because of the phase errors in the source visibility data, it is, of course, possible only to remove the response to the

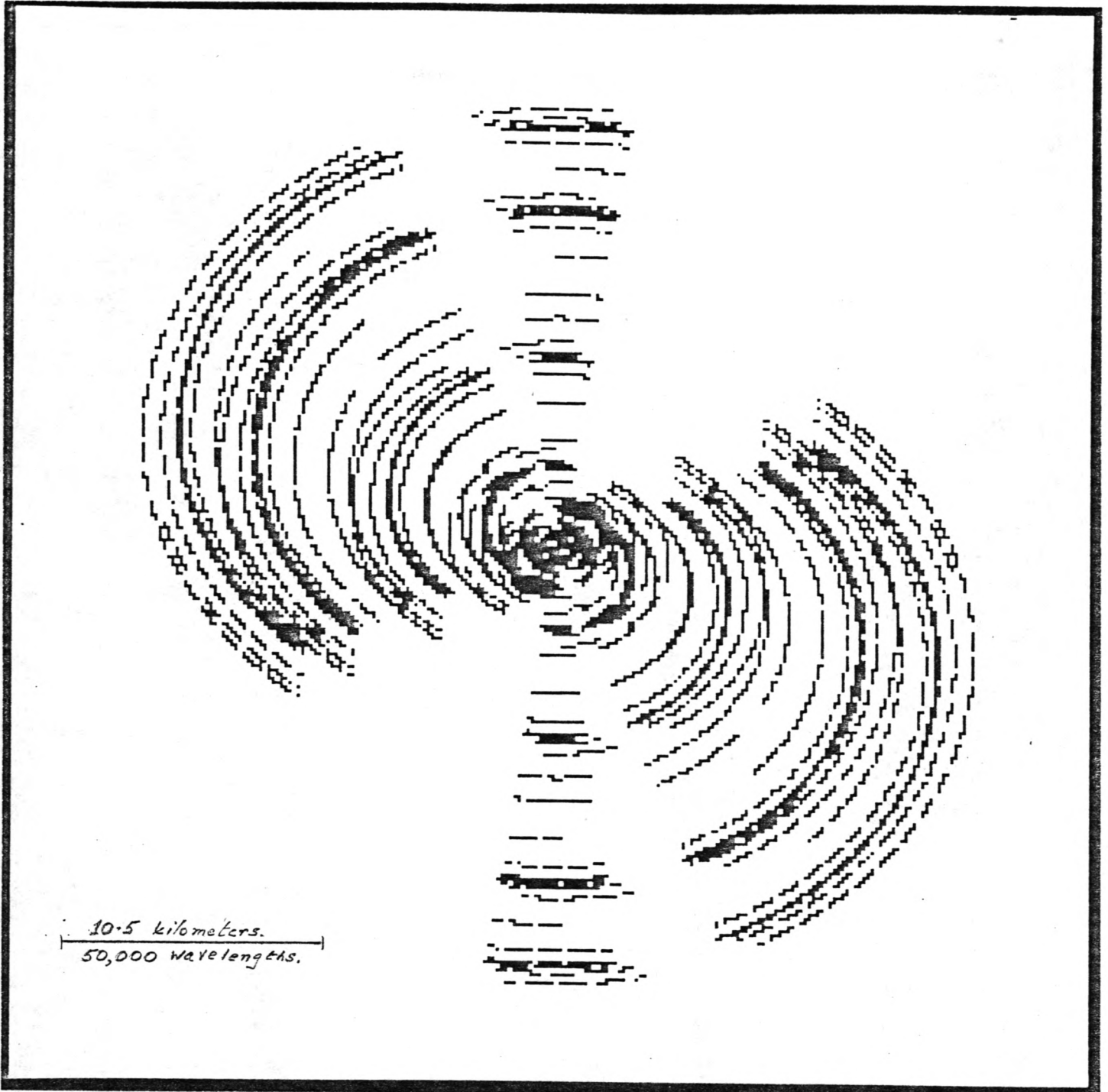


Figure 1: The spacial frequency coverage in the  $(u,v)$ -plane for the observation of 0537+531. The  $u$ -axis is horizontal.

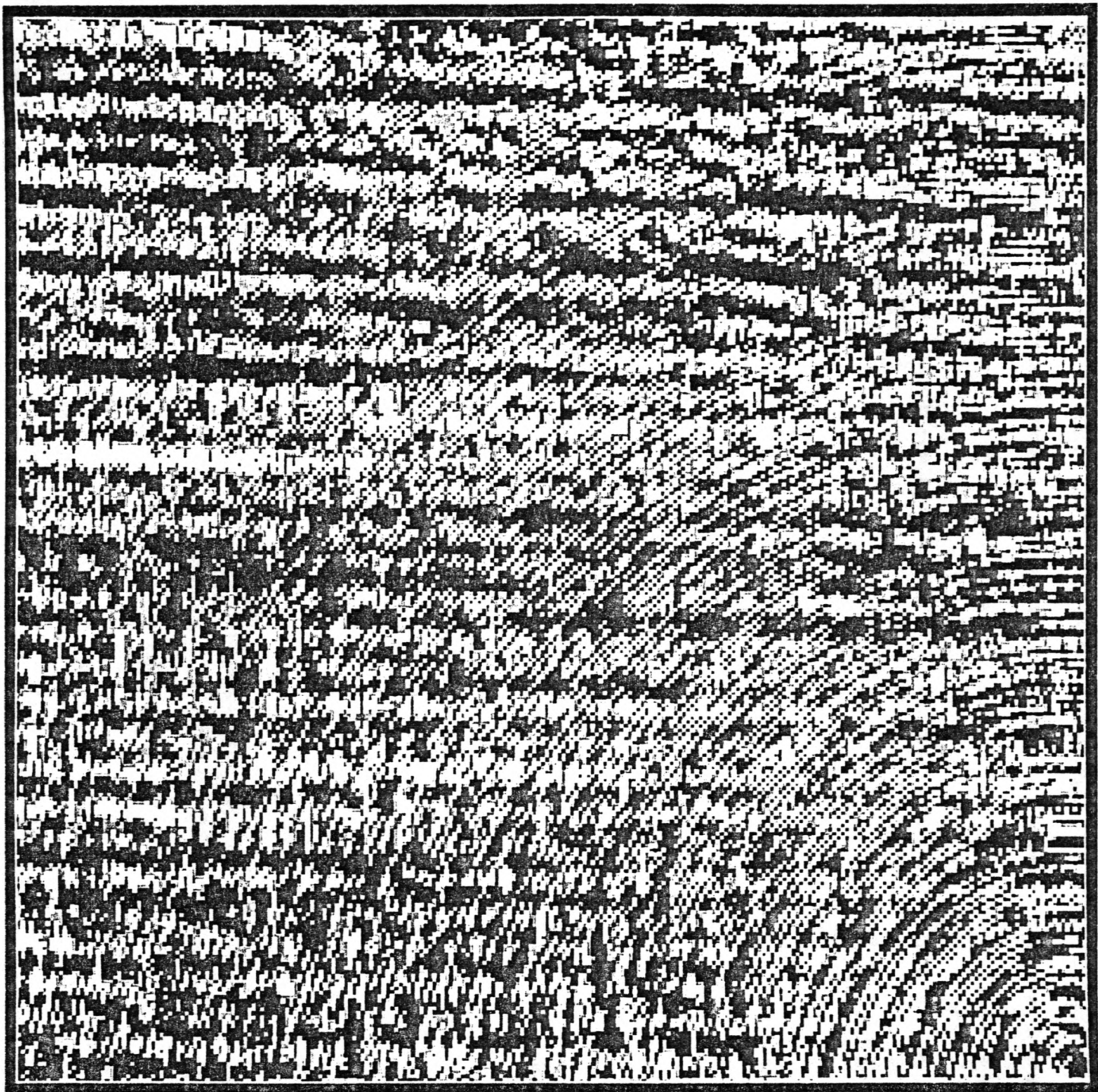


Figure 2: Northeast quadrant of a  $512 \times 512$  map with  $\Delta x = 3$  arcsec. The response to the source 0537+531 has not been subtracted and is centered in the lower right corner.

source down to some level below which a noise-like component remains. In the present case this component appeared to be of the order of 1 mJy rms, compared with about 730 mJy for the flux density of 0537+531. In a map with  $\Delta u = 1611$  wavelengths (dimension 128 and  $\Delta x = 1''$ ) the interference was no longer reliably distinguishable against a background fluctuation of the order of 2 mJy rms. In retrospect, it may have been better to map a weaker source or even blank sky.

One map was made using Gaussian interpolation of the visibility data, and the results for it are given in the bottom row of Table I. The convolving function in the  $(u,v)$ -plane for the VLA program MAKMAP is

$$\exp[-\frac{1}{2}(u/n_c \Delta u)^2] \exp[-\frac{1}{2}(v/n_c \Delta v)^2], \quad (1)$$

and in the present case the value  $n_c = 1$  was used. Gaussian convolution is not considered in VLA EM No. 183, but with expression (1) above the equivalent expression for the rms interference amplitude given in equation (4) of VLA EM No. 183 is

$$F1 = \left[ \frac{2}{\pi} \int_0^{\infty} \exp-(2\pi\Delta u\phi\cos\delta)^2 d\phi \right]^{\frac{1}{2}} = \left( \frac{1}{\pi\Delta u\cos\delta} \right)^{\frac{1}{2}} \left( \frac{1}{4\pi} \right)^{\frac{1}{4}} \quad (2)$$

which is the result for cell averaging multiplied by  $\left(\frac{1}{4\pi}\right)^{\frac{1}{4}}$ .

The agreement between the observed and expected ratios of the interference amplitudes given in Table I is good for the cell-averaging cases, but, for reasons not understood, it is not quite so good for the Gaussian interpolation.

To estimate the gain in the far side lobes of the antennas from the interference amplitude we note that the rms amplitude of the interference, expressed as a fraction of the response to a point source of unit flux density, is given by

$$R = \left(\frac{I}{B}\right) \left(\frac{G_S}{G_M}\right) \left(\frac{1}{\pi \Delta u \cos \delta}\right)^{\frac{1}{2}} \left(\frac{\alpha}{2}\right)^{\frac{1}{2}} \quad (3)$$

In the above equation the first factor on the right-hand side is the strength of the interfering signal,  $I$ , divided by the receiving bandwidth,  $B$ . The second factor is the ratio of the gain of the antennas in the far side lobes to that in the main beam. The third factor is the effect of fringe-frequency averaging derived in VLA EM No. 183. In the fourth factor,  $\alpha$  is the fraction of the total number of baselines for which the  $u$  goes through zero when the observations are in progress, and  $\frac{1}{2}$  takes account of the fact that for a point source the components in the map resulting from the two oppositely polarized channels add directly, but for the interference they combine as the sum of the squared amplitudes. For the case with the highest interference-to-noise ratio in Table I we have  $R = 5.32$  mJy for  $\Delta u = 134$  wavelengths, and  $I = -125.7$  dB  $\text{Wm}^{-2}$ ,  $B = 12$  MHz,  $G_M = 6.99 \times 10^4$ ,  $\delta = 53.2^\circ$ , and  $\alpha = 0.36$ . (The fringe frequency went through zero when good data was being recorded on 0537+531 for only 33 out of the 91 baselines.) These values give  $G_S = -22$  dB an uncertainty of about  $\pm 4$  dB. This figure represents an average of the gains in the transmitter direction at times when  $u = 0$  for the 33 baselines.

Approximately 80% of the baselines for which the fringe frequency went through zero involved antennas on the west arm. Most of these baselines therefore have azimuths similar to that of the west arm, for which  $u = 0$  occurred at an hour angle of  $+69^\circ$ , i.e., during the last hour of the observations. At that time the antennas were pointing towards the west, in almost the opposite direction to the transmitter. This appears to be the main reason for the rather low value of  $-22$  dB for the side lobe response. To examine this point further, the visibility amplitude is plotted as a function of time for two short baselines, 244 and 181 metres. The maximum possible fringe frequency for these baselines was 0.08 Hz, so that for most of the time the fringe amplitudes should be only marginally reduced by the 10-second averaging of the visibility data. The amplitudes of the

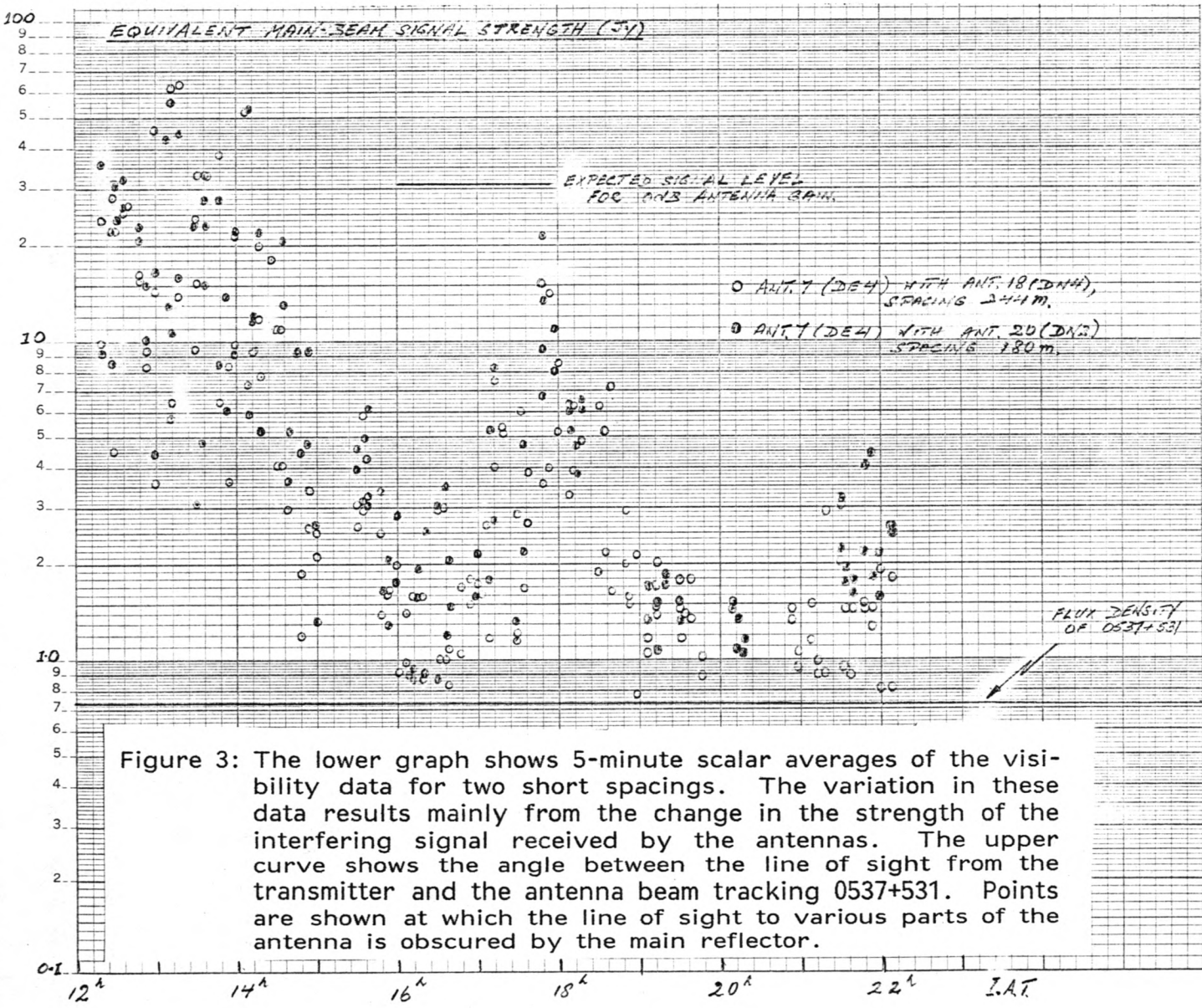
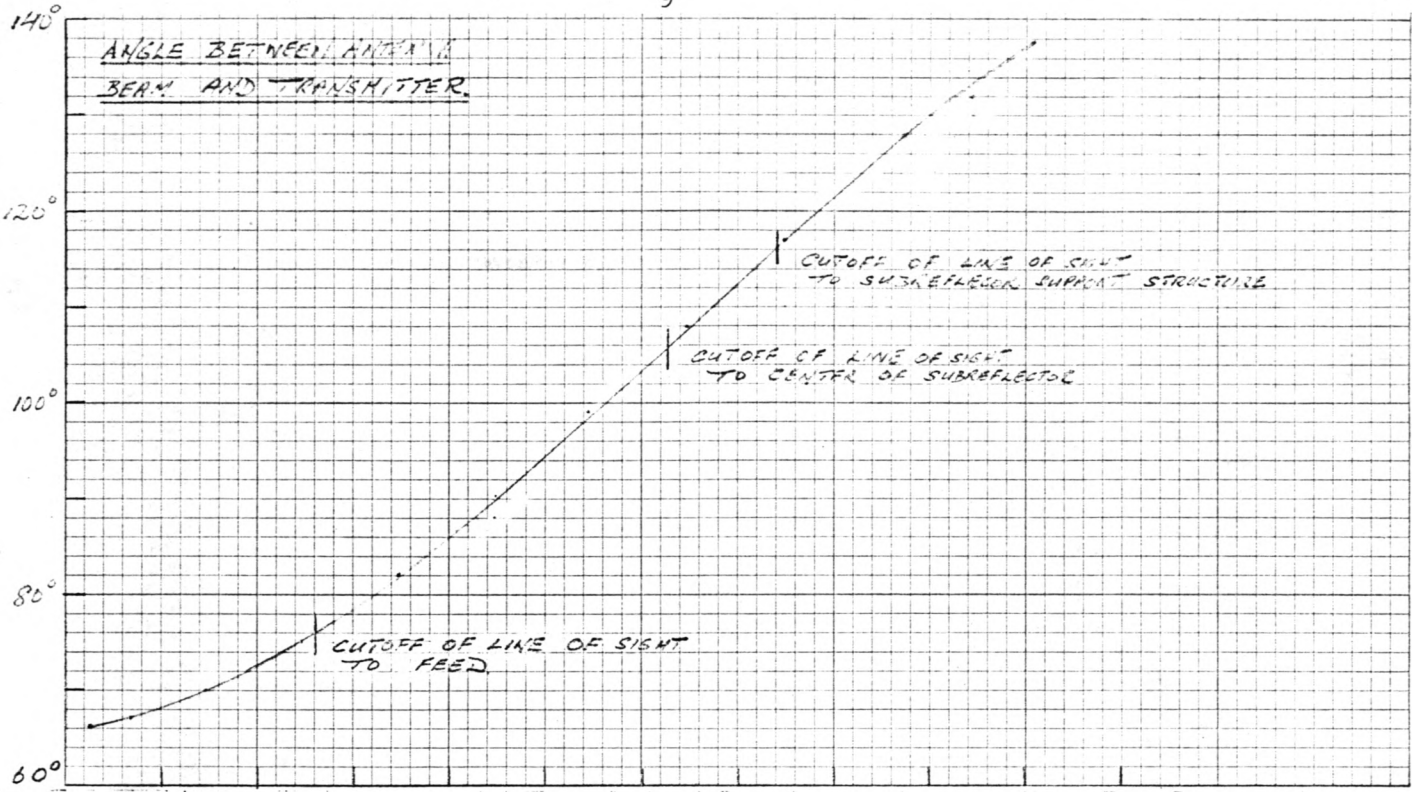


Figure 3: The lower graph shows 5-minute scalar averages of the visibility data for two short spacings. The variation in these data results mainly from the change in the strength of the interfering signal received by the antennas. The upper curve shows the angle between the line of sight from the transmitter and the antenna beam tracking 0537+531. Points are shown at which the line of sight to various parts of the antenna is obscured by the main reflector.

10-second records were averaged for 5-minute intervals and plotted as a function of time in Figure 3. The amplitude scale is the equivalent flux density for a signal in the main beam, and a level of 32 Jy corresponds approximately to an antenna gain of 0 dB. This level occurred near the beginning of the run, and as the antennas tracked over to the west the level fell. The source being mapped, 0537+531, provides a contribution of approximately 0.73 Jy in the main beam, so a level of 1 Jy corresponds to a drop of about 20 dB in the level of the interfering signal. It appears, therefore, that around 21 hours IAT the side lobe response in the direction of the transmitter was something of the order of -20 dB, which is consistent with the value of  $G_s$  obtained above. The upper curve in Figure 2 shows the angle between the main beam of the antennas and the transmitter. The high signal levels near the start of the run occurred when there was a direct line of sight from the transmitter to the feed at the antenna vertex. At about 1800 IAT, just before the Cassegrain subreflector was obscured by the main reflector, the signal level rose. This is the point at which a spillover side lobe would occur with a prime-focus feed, and presumably a similar effect occurs with the Cassegrain system. The lowest signal levels occurred after the reflector had obscured all of the structure on the front side of the antenna. The peak near 2200 IAT may result from reflection of the transmitted signal from the back of one antenna into the aperture of another, for the closely spaced antennas near the array center. At that time the azimuth of the source was about  $310^\circ$ , which is roughly opposite the azimuths of the transmitter at  $106^\circ$  and the east arm at  $115^\circ$ .

#### 4.0 CONCLUSIONS

The array behavior discussed in VLA EM No. 183 is based on the assumption that a steady signal level would be received through the far side lobes of the antennas. In fact, the side lobes show considerable variation and angular structure, as indicated in Figure 3. Reflections from other antennas may also complicate the situation for short spacings. The effect of averaging on the interfering signal

is therefore unlikely to be predictable with an accuracy better than a few decibels. With this in mind, one can conclude that the results presented above confirm the approach used in the earlier memorandum. It is hoped to make a further independent study of the far side lobe gain of the antennas to further check the present results and to provide a more accurate basis for prediction of harmful interference levels.

The probability distribution of the amplitudes for two of the maps is shown in Figure 4. These amplitudes result mainly from the interference. The curves show few high amplitude values, and fall to less than 1% probability for amplitude levels between two and three times the rms value. A criterion for the maximum acceptable rms interference level of  $10^{-1}$  times the rms noise should therefore be quite satisfactory, since the probability of an interference level greater than the rms noise would be extremely small. The use of  $10^{-2}$  times the rms noise in VLA EM No. 183 appears to be very conservative.

In considering the results discussed above, several procedures come to mind which should be helpful if the presence of an interfering signal cannot be avoided. Removal of data points for which  $u$  is close to zero would be effective, but would produce unwanted side lobes on the synthesized beam. In some cases it may be possible to remove such side lobes by further data analysis such as the use of the CLEAN algorithm. Alternatively it may be preferable only to remove data when both  $u$  is small and the side lobe gain in the direction of the interfering source is high. With a two-dimensional array like the VLA this is a possible procedure since baselines cover a wide range of azimuths, and for any source  $u$  goes through zero at many different hour angles. After averaging and interpolation in the  $(u,v)$ -plane, the interference amplitude varies with  $u$  approximately as the Fourier transform of the convolving function. Editing of data with low values of  $u$  should be more effective with Gaussian convolution than with cell averaging since a Gaussian envelope in the  $(u,v)$ -plane falls to zero more rapidly than a sinc function. It is clearly

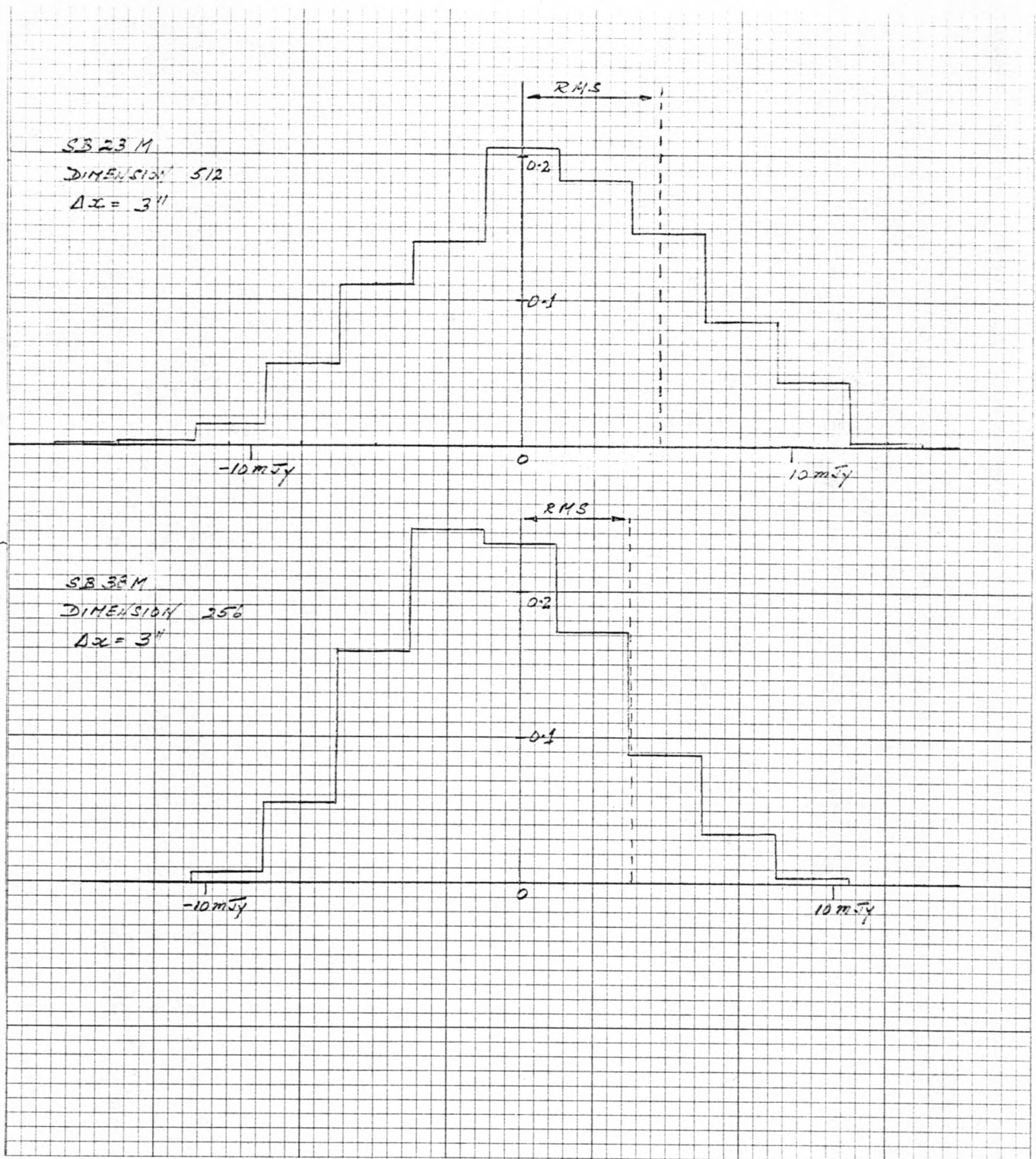


Figure 4: The amplitude probability distribution for two maps. The amplitudes result mainly from the interfering signal but a smaller component is present which includes the residual effects of the source and the system noise.

beneficial to keep  $\Delta u$  as large as possible, and it might therefore in some cases be worthwhile to construct large-field maps as combinations of smaller ones. Finally, it is obviously desirable to minimize the effects of interference in the calibration observations, and this suggests the use of more than one calibration source so that data for which  $u$  is small, or the side lobes in the transmitter direction large, can be eliminated.

#### ACKNOWLEDGMENT

We should like to thank Dr. W. P. Winn and Dr. C. B. Moore of New Mexico Institute of Mining and Technology for kindly allowing us to use the Langmuir Laboratory as a site for the transmitter.

TABLE I

VARIATION OF RMS INTERFERENCE LEVEL WITH INTERPOLATION PARAMETERS

Mapname	Interpolation Method	Dimension	$\Delta x$ (arcsec)	$\Delta u$ (wavelengths)	RMS Interference Level		
					Measured (mJy)	Measured (ratio)	Expected (ratio)
SB23M	cell averaging	512	3	134	5.3	1.0	1.0
SB38M	cell averaging	256	3	268	3.6	0.67	0.71
SB26M	cell averaging	256	1.5	536	2.5	0.47	0.50
SB40M	Gaussian convolution	512	3	134	3.6	0.67	0.53